Journal of Inorganic and Organometallic Polymers and Materials (2018) 28:1294–1298
https://doi.org/10.1007/s10904-018-0787-x

Synthesis and Luminescence Properties of Immobilized Europium β-CD Complexes on Silica

Wen Jun Zhang[1] · Yi Chen[1] · Shao Pei Zhang[1] · Shao Kang Tang[1] · Xue Qing Chen[1] · Guang Yu Cui[1]

Received: 20 November 2017 / Accepted: 7 January 2018 / Published online: 11 January 2018

Abstract
Functionalized silica gel organic–inorganic hybrid materials based on covalently grafted lanthanide coordinations onto organosilicone have been the subject of intense study due to their superior physicochemical properties. However, it cannot be assumed that all the primary guest molecules can be directly covalent-grafted onto the host that prevents H_2O molecules from coordinating with the central ion; the introduction of a medium could be useful in this regard. In the present work, a medium β-cyclodextrin (β-CD) was employed, and by sol–gel and molecular assembly processes, immobilization of a europium–β-CD inclusion on silica and the preparation of a novel fluorescent polymeric hybrid material β-CD–TESPIC–TTA–Eu were achieved. This research shows that β-CD can prevent the H_2O molecules from coordinating with the central ion Eu^{3+} (inclusion). The novel hybrid material has an amorphous and homogeneous network surface and exhibits excellent film-forming properties, bright-red light emission that is dominated by the $^5D_0 \rightarrow {}^7F_2$ transition of Eu^{3+}, and a lifetime of 0.44 ms.

Keywords Molecular assembly · Sol–gel preparation · Polymeric europium complexes · Optical materials

1 Introduction

In the past few decades, research groups have incorporated lanthanide complexes into organosilicone to overcome the physicochemical disadvantages of luminescent rare earth complexes, by preparing a series of outstanding so-called organic–inorganic host–guest silica gel hybrid materials [1–5]. Among these advances, the direct covalent grafting of a primary ligand onto an inorganic host matrix can be considered a superior approach [6–8]. However, several problems remain regarding this approach. One cannot assume that all the primary ligands can be directly covalent-grafted onto the host matrix; H_2O molecules might need to be prevented from coordinating with the central coordination ion.

β-Cyclodextrin (β-CD) has a "bucket-shaped" appearance (Fig. 1) with a hydrophobic inner cavity, which shows a remarkable ability to form host–guest inclusion complexes [9, 10]. The active group –OH of β-CD can react with the –NCO of organosilicone to construct a series of multifunctional precursors [11–13], which might be able to efficiently solve the above issue.

Based on these considerations, in this paper, we present a novel path to tether lanthanide complexes onto Si–O–Si composite matrices by employing β-CD. The hydroxyl of β-CD reacted with the –NCO of the 3-isocyanatopropyltriethoxysilane (TESPIC) to create the precursor host. The guest lanthanide complexes (between 2-thenoyltrifluoroacetone and europium) were inserted into the β-CD cavity to form europium β-CD inclusions. Then, the hybrid material based on Si–O–Si composite matrices were finally obtained via the sol–gel and molecular assembly approaches. The resulting hybrid material was characterized, and the luminescence properties were studied in detail.

Electronic supplementary material The online version of this article (https://doi.org/10.1007/s10904-018-0787-x) contains supplementary material, which is available to authorized users.

✉ Wen Jun Zhang
wjzhang@hebut.edu.cn

[1] School of Chemical Engineering, Hebei University of Technology, Tianjin 300130, China

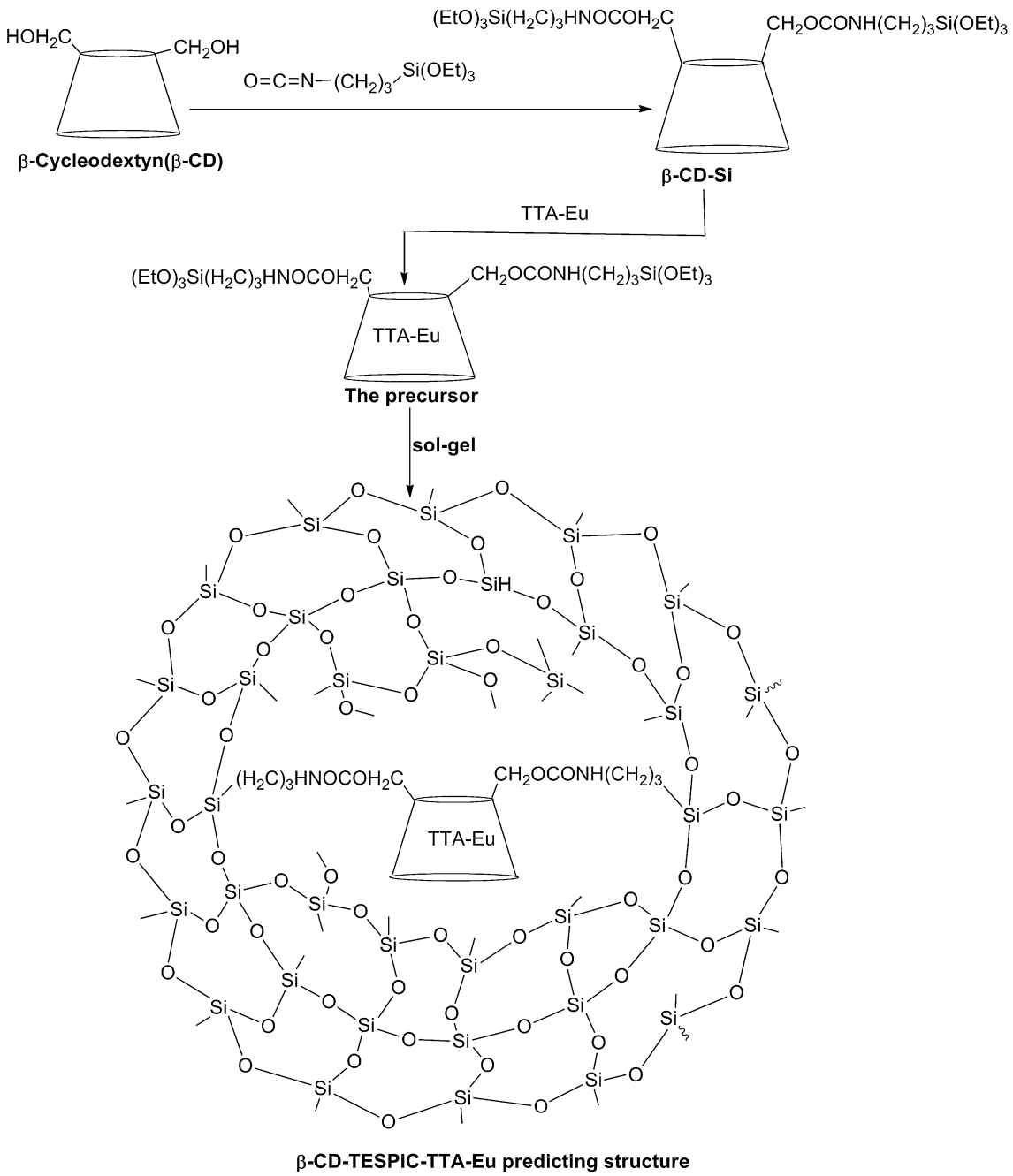

Fig. 1 Synthesis schematic and the predicted structure of β-CD–TESPIC–TTA–Eu

2 Experimental

2.1 Materials

Analytical-grade europium oxide, hydrochloric acid, absolute alcohol, and *N,N*-dimethylformamide (DMF) were purchased from Tianjin Chemical Co. Ltd, and utilized without further purification. 2-Thenoyltrifluoroacetone (TTA; 98%), β-cyclodextrin (β-CD; 98%), 3-isocyanatopropyltriethoxysilane (TESPIC; 95%), and ammonium hydroxide (25%) were purchased from Beijing HWRK Chemical Co. Ltd. and used as received. A $EuCl_3$ (0.1 mol/L) ethanol solution was obtained by dissolving Eu_2O_3 in an ethanol solution.

2.2 Synthesis of β-CD–TESPIC–TTA–Eu

The entire reaction procedure was conducted in an argon atmosphere (Fig. 1). Typically, TESPIC (1 mmol) was added dropwise with stirring into the mixture (1.0 mmol β-CD, 20 mL DMF), and the mixture was heated to 70 °C to reflux for 7 h to obtain β-CD–Si. After preparing β-CD–Si, 1.0 mmol TTA and 0.34 mmol of $EuCl_3$ were injected into the β-CD–Si reaction system. The resulting mixture was kept at 70 °C to reflux for an additional 5 h to synthesize the host–guest inclusions. Then, hydrochloric acid was added dropwise into the reaction system and refluxed for 3 h (sol–gel process). The obtained sample was vacuum dried at 50 °C and denoted as β-CD–TESPIC–TTA–Eu.

2.3 Characterization

Fourier transform infrared (FT-IR) absorption spectra were measured using a FT-IR Equino x22 Bruker spectrometer in the range 4000–400 cm^{-1}. In one experimental condition, namely, at a voltage of 45 kV and an electric current of 100 A, the X-ray powder diffraction (XRD) patterns were obtained in the 2θ range 5°–90° using a Japan Rigaku-Dmax 2500 X-Ray diffractometer with CuK_α radiation (λ = 0.1541844 nm) at a scan rate of 100/min. The morphology of the sample was examined using a scanning electron microscope (SEM; FEI Nova Nano SEM450) at an acceleration voltage of 15 kV. Thermal gravimetric analysis (TGA) was performed using a Thermal Analysis SDT2960 apparatus under a nitrogen atmosphere. The temperature range for heating was 30–1000 °C, and the heating rate was 10 °C min^{-1} in nitrogen. The steady-state luminescence spectra and lifetime measurements were recorded with an Edinburgh FS920P near-infrared spectrometer with a 450-W xenon lamp as the steady-state excitation source.

3 Results and Discussion

3.1 Infrared Spectroscopic Analysis

The hybrid materials are part of a complicated system; however, it is possible to monitor the reaction process based on functional groups. The FTIR spectra of β-CD, TESPIC, β-CD–TESPIC, and β-CD–TESPIC–TTA–Eu are shown in Fig. 2. The adsorption bands at 3377, 2927, 1646, 1158, and 1031 cm^{-1} emerged, which separately correspond to the stretching vibration of –OH, $–CH_2–$, the glucose ring, and C–O–C in the β-CD [14, 15]. The adsorption bands at 1663 and 1554 cm^{-1} are assigned to the C=O stretching and N–H bending vibrations of the amide bond, respectively. The stretching vibration peaks at 2276 cm^{-1} for O=C=N from TESPIC disappeared in the case of β-CD–TESPIC,

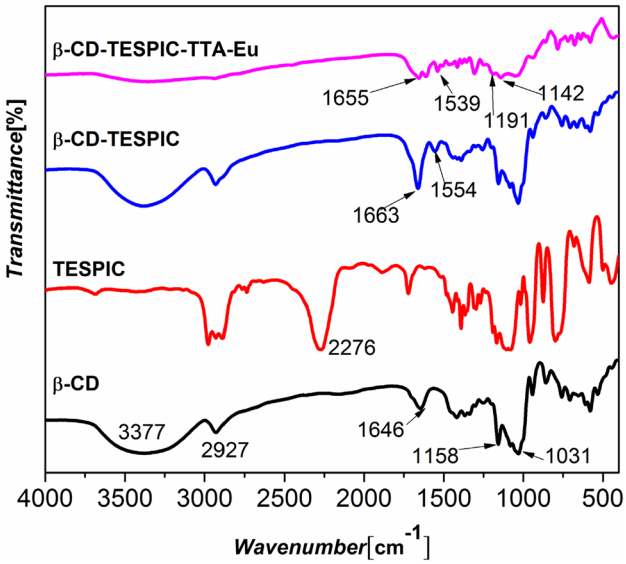

Fig. 2 FTIR spectra of β-CD, TESPIC, β-CD–TESPIC, and β-CD–TESPIC–TTA–Eu

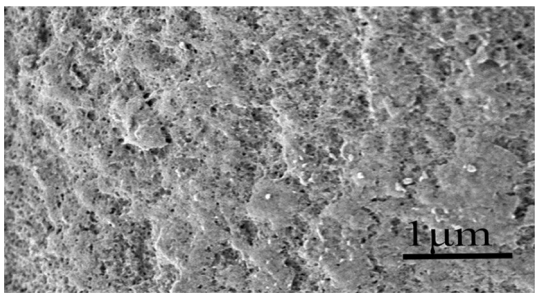

Fig. 3 SEM image of β-CD–TESPIC–TTA–Eu

indicating the completion of the grafting reaction; in other words, TESPIC was successfully grafted onto β-CD. Furthermore, in the spectrum of β-CD–TESPIC–TTA–Eu, the adsorption bands assigned to the C=O stretching and N–H bending vibrations shift to 1655 and 1539 cm^{-1}, and the typical C–Si and Si–O–Si stretching vibrations appear at about 1191 and 1142 cm^{-1}, respectively, which confirm the completion of sol–gel polycondensation and molecular assembly [16].

3.2 Powder X-ray Diffraction and Scanning Electron Microscopy Analysis

As shown by the XRD pattern, the hybrid material β-CD–TESPIC–TTA–Eu is amorphous (Fig. S1). The surface morphology of the obtained hybrid material was studied using SEM. The SEM image (Fig. 3) reveals that the hybrid is composed of a compacted network. The uniform

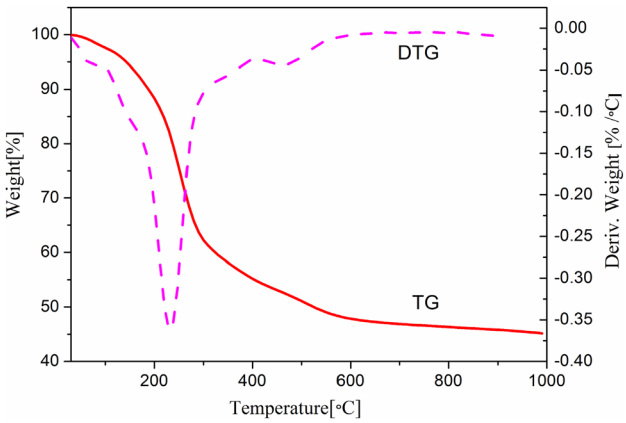

Fig. 4 TG/DTG curve of β-CD–TESPIC–TTA–Eu with a heating rate of 10 °C min^{-1} in a nitrogen atmosphere

frameworks on the surface suggest that a homogeneous molecular-based material was obtained because of strong covalent bonds in the Si–O–Si networks (via molecular assembly) that belong to a complicated and large molecular system.

3.3 TG/DTG Curves

Thermogravimetric analysis of β-CD–TESPIC–TTA–Eu was carried out (Fig. 4). The overall thermal treatment process can be divided into four stages as the temperature increases.

From 30 to 100 °C, a thermal decomposition peak center at 80 °C and weight loss of approximately 2.4 wt% are seen, which can be ascribed to the release of residual ethanol from the β-CD–TESPIC–TTA–Eu surface. From 100 to 450 °C, the weight loss was approximately 44.5 wt% and a strong thermal absorption decomposition peak (center at 250 °C) can be observed on the DTG curves of β-CD–TESPIC–TTA–Eu, which is attributed to the decomposition of β-CD rings and carbon chains [17] and exposure of TTA–Eu to the hot environment. From 450 to 610 °C, the weight loss was approximately 16.4 wt% and a broad thermal absorption decomposition peak (peak center at 510 °C) can be observed, which indicates that the fluorescent TTA–Eu complex was damaged [18]. When the temperature was above 610 °C, the TG/DTG curves of the hybrid materials were parallel.

The results of the analysis show that water molecules are not present and that the β-CD ring can prevent them from coordinating with the (inclusion) central ion Eu^{3+} and avoiding fluorescence quenching because of the –OH group vibration.

3.4 Optical Properties of β-CD–TESPIC–TTA–Eu

The luminescence properties of β-CD–TESPIC–TTA–Eu were studied. The characteristic excitation and emission spectra of the hybrid material are presented in Fig. 5. The excitation spectrum for the hybrid material was obtained by monitoring the most intense $^5D_0 \rightarrow {}^7F_2$ transition of Eu^{3+} at 612 nm. The excitation spectrum shows a broad band from 240 to 460 nm with a center peak at 381 nm, which is ascribed to the organic ligand π–π transitions, and a much weaker peak at 468 nm, corresponding to the $^7F_0 \rightarrow {}^5D_2$ transition of Eu^{3+}; this indicates that the process of obtaining the Eu^{3+} excited state via the excitation of the organic ligand is much more efficient than the direct excitation of the Eu^{3+} energy level.

For excitation in the ligand absorption band (381 nm), only the characteristic emission lines arising from the $^5D_0 \rightarrow {}^7F_j$ (j = 0,1, 2, 3, and 4) transitions of Eu^{3+} were observed; no broad emission band from organic ligands in the blue region was detected, indicating that effective energy transfer could occur from the ligands to central Eu^{3+}. In addition, the red emission at 612 nm from the electronic dipole transition $^5D_0 \rightarrow {}^7F_2$ has the strongest intensity. The calculated intensity ratio I_2/I_1 of the $^5D_0 \rightarrow {}^7F_2$ and $^5D_0 \rightarrow {}^7F_1$ transitions of Eu^{3+} indicates that the Eu^{3+} site is situated in an environment without inversion symmetry, implying the coordination bond formation between Eu^{3+} and TTA [6–8]. The hybrid material β-CD–TESPIC–TTA–Eu is liquid at room temperature. We evenly applied a sample on quartz glass, obtained a continuous, unbroken, uniform, and transparent thin film. The sample and film emit a bright red luminescence upon radiation with ultraviolet light at 254 and 365 nm (Fig. S2).

The luminescence decay curve of the $^5D_0$ state for β-CD–TESPIC–TTA–Eu is fitted with single exponentials (Fig. 6). The $^5D_0$ excited-state lifetime of Eu^{3+} in β-CD–TESPIC–TTA–Eu was determined to be 0.44 ms;

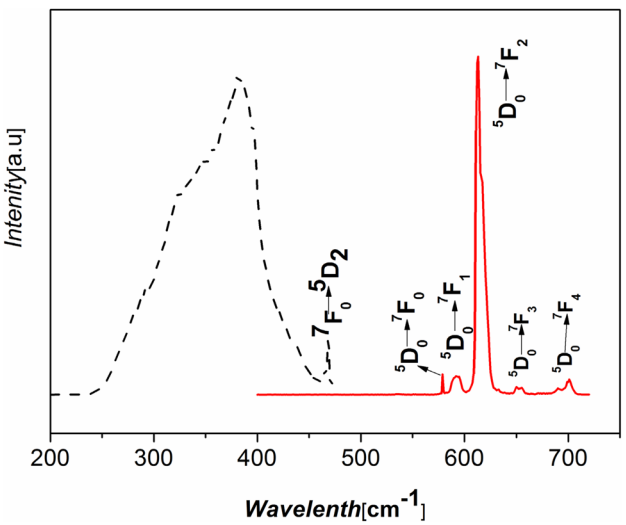

Fig. 5 Excitation (dotted line) and emission (solid line) spectra of the hybrid β-CD–TESPIC–TTA–Eu material

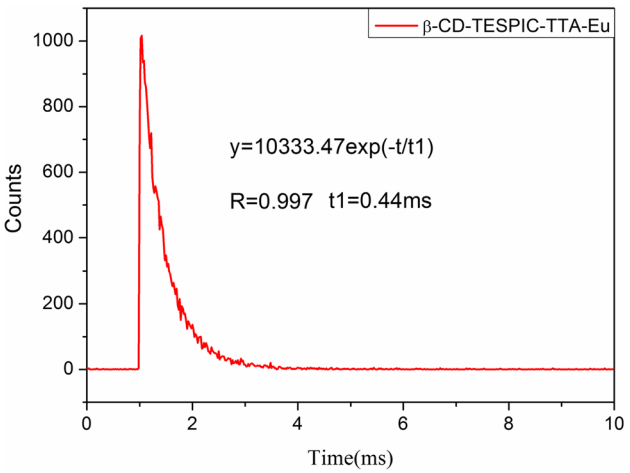

Fig. 6 $^5D_0$ lifetime of Eu^{3+} in β-CD–TESPIC–TTA–Eu; $\lambda_{ex} = 381$ nm, $\lambda_{monitored} = 613$ nm

this is much longer than the lifetime of $[Eu(TTA)_3]\cdot 2H_2O$ (t = 0.333 ms) [6–8]. It is possible that (a) the hydrophobic inner cavity of β-CD hinders H_2O molecules from coordinating with the Eu ions, (b) the relatively rigid structure of silica gel limits prohibitive nonradiative transitions, and (c) the leaching of the photoactive molecules and clustering of the emitting centers could be avoided.

4 Conclusion

In summary, by employing β-CD as the medium and immobilizing the europium β-CD inclusions in silica, we developed a novel method to assemble a luminescent lanthanide organic–inorganic hybrid material based on the composite matrices of Si–O–Si networks. This method was realized using the hydroxyl group of β-CD that reacted with the –NCO of TESPIC, inserting lanthanide complexes $[Eu(TTA)_3]$ into the β-CD cavity and resulting in sol–gel polycondensation and molecular assembly. The obtained material possesses a uniform microstructure and exhibits excellent fluorescence performance and film-forming properties, which suggests that it may be applied in optical devices. In addition, this facile strategy to tether lanthanide complexes to organic–inorganic Si–O–Si networks may be used to prevent the guest molecule from being directly covalently grafted onto the host.

Acknowledgements The project was supported by Hebei Education Foundation (ZD2017214).

References

1. A.C. Franville, D. Zambon, R. Mahiou, S. Chou, Y. Troin, J.C. Cousseins, J. Alloys Compd. **275–277**(98), 831–834 (1998)
2. Y.-F. Shao, B. Yan, Z.-Y. Jiang, RSC Adv. **2**(24), 9192 (2012). https://doi.org/10.1039/c2ra21605a
3. J.-N. Hao, B. Yan, New J. Chem. **38**(8), 3540 (2014). https://doi.org/10.1039/c4nj00466c
4. Y. Li, X. Ge, X. Pang, X. Yu, X. Zhen, L. Geng, Y. Wang, Mater. Lett. **152**, 170–172 (2015). https://doi.org/10.1016/j.matlet.2015.03.127
5. Q. Xu, Z. Li, M. Chen, H. Li, CrystEngComm **18**(1), 177–182 (2016). https://doi.org/10.1039/c5ce01664a
6. X. Guo, H. Guo, L. Fu, H. Zhang, L.D. Carlos, R. Deng, J. Yu, J. Photochem. Photobiol. A **200**(2–3), 318–324 (2008). https://doi.org/10.1016/j.jphotochem.2008.08.016
7. X.F. Qiao, B. Yan, Inorg. Chem. **48**(11), 4714–4723 (2009). https://doi.org/10.1021/ic8017776
8. X. Chen, P. Zhang, T. Wang, H. Li, Chemistry **20**(9), 2551–2556 (2014). https://doi.org/10.1002/chem.201303957
9. X. Sun, S. Sui, C. Ference, Y. Zhang, S. Sun, N. Zhou, W. Zhu, K. Zhou, J. Agric. Food Chem. **62**(35), 8914–8918 (2014). https://doi.org/10.1021/jf5027873
10. P.d..P. Menezes, M.R. Serafini, Y.M.B.G. de Carvalho, D.V. Soares Santana, B.S. Lima, L.J. Quintans-Júnior, R.N. Marreto, T.M. de Aquino, A.R. Sabino, L. Scotti, M.T. Scotti, S. Grangeiro-Júnior, A.A. de Souza Araújo, J. Mol. Struct. **1125**, 323–330 (2016). https://doi.org/10.1016/j.molstruc.2016.06.062
11. S. Hu, Y. Xu, D. Jiang, D. Wu, Y. Sun, F. Deng, Thin Solid Films **518**(1), 348–354 (2009). https://doi.org/10.1016/j.tsf.2009.06.024
12. S. Hu, D. Yang, Y. Xu, D. Wu, Y. Sun, Mater. Chem. Phys. **114**(2–3), 868–873 (2009). https://doi.org/10.1016/j.matchemphys.2008.10.071
13. C. Sun, C. Li, R. Qu, Y. Zhang, Z. Bingdong, Y. Kuang, Chem. Eng. J. **240**, 369–378 (2014). https://doi.org/10.1016/j.cej.2013.11.092
14. S.P. Zhang, H.O. Song, Chem. J. Chin. Univ. **33**(6), 1214–1219 (2012)
15. Y. Yang, F. Gao, X. Cai, X. Yuan, S. He, F. Gao, H. Guo, Q. Wang, Biosens. Bioelectron. **74**, 447–453 (2015). https://doi.org/10.1016/j.bios.2015.06.018
16. Y.F. Shao, B. Yan, Z.Y. Jiang, RSC Adv. **2**(24), 9192–9200 (2012)
17. Y. Wang, C.W. Jin, S.M. He, N. Ren, J.J. Zhang, J. Mol. Struct. **1125**, 383–390 (2016)
18. Y. Li, B. Yan, Y. Li, J. Solid State Chem. **183**(4), 871–877 (2010). https://doi.org/10.1016/j.jssc.2010.02.006